NUCLEAR MAGNETIC RESONANCE STUDY OF ACETIC ACID PERMEATION OF LARGE UNILAMELLAR VESICLE MEMBRANES

J. R. ALGER AND J. H. PRESTEGARD, *Department of Chemistry, Yale University, New Haven, Connecticut 06520 U.S.A.*

ABSTRACT The permeation of acetic acid through large unilamellar phospholipid vesicle membranes has been investigated using the unique capability of nuclear magnetic resonance to characterize flow under pseudo-equilibrium conditions. Two types of experiments have been employed: total line shape analysis and selective population transfer. These techniques are sensitive to permeation on time scales ranging from 0.001 to 10.0 s. The permeation rate dependence on pH and acetic acid concentration indicates that the neutral acetic acid monomer is the dominant permeant species with a permeation coefficient of $5 \pm 2 \times 10^{-4}$ cm/s. Mechanisms of permeation and the applicability of nuclear magnetic resonance methodology are discussed.

INTRODUCTION

Measurement of permeation rates of small molecules through model membranes has been an active area of scientific research for several decades (1). Studies have usually involved observing transient solute flow driven by an experimentally imposed gradient in electrochemical potential or hydrostatic pressure. The model membranes used in these studies have included black lipid films (2,3), liposomal dispersions (1), and small unilamellar phospholipid vesicles (1). The data acquired from such work has had far-reaching significance in the understanding of active and passive transport mechanisms in biological membranes.

Despite the value of these studies, both the techniques employed and model membranes chosen present limitations. Black lipid membranes have a geometry convenient for conductivity studies, but the lipid composition of the membrane is often restricted, and solvent residues often remain in the membrane. The dimensions and curvature of the black lipid membranes rarely resemble biological membranes. Multilamellar liposomes can more closely resemble biological membranes in dimension and composition, and have been extensively used to study permeation of fluorescent or radio labeled molecules. Experimental control of forces that drive permeation is difficult in liposomes, and correlation of measured net flux with permeation of a single bilayer is difficult to establish. Small unilamellar vesicles prepared by sonication or solvent injection offer a well-defined single bilayer across which the flux of a permeant solute can be measured, but have been available with diameters no larger than 500 Å. Permeation data for small unilamellar vesicles may be complicated by difficulties associated with

Various aspects of this work were presented at the 19th Experimental Nuclear Magnetic Resonance Conference in Blacksburg, Va., 16–20 April 1978, and at the 23rd Annual Meeting of the Biophysical Society in Atlanta, Ga., 28 February 1979.

assigning bulk phase properties to the small internal volume. Furthermore, permeation data may not be pertinent to natural membranes of larger radius of curvature.

Above and beyond problems associated with choice of appropriate model membrane systems, most classical techniques require physical manipulations to measure the solute concentrations in the aqueous compartments, and to impose the gradient that drives the solute permeation. Often the manipulations introduce long dead times that prohibit the detailed observation of rapid permeation. Measurement of solute concentrations at points distant from the membrane requires that the time necessary for the molecule to diffuse through the unstirred layer between the point of observation and the membrane surface be included in the data analysis. For rapidly permeating molecules this unstirred layer diffusion can rate limit the net observed flux and cause the experiment to be insensitive to membrane permeation (4). Many of these limitations can be relaxed by the introduction of new preparative and analytical methods. The large unilamellar vesicles, which have been recently prepared by the ether injection procedure of Deamer and Bangham (5), offer several advantages as a model system for the study of solute permeation. They are similar to intracellular organelles, such as mitochondria, in dimension and radius of curvature, and are very nearly unilamellar. In this paper, we present data on permeation of small solute molecules through unilamellar vesicle membranes prepared by the ether injection procedure.

We also introduce nuclear magnetic resonance techniques, which offer significant advantages over more conventional techniques, for the study of solute permeation. Spectroscopic techniques that give distinct signals for interior and exterior spaces eliminate the need for physical separations, and reduce the effective distances from the membrane at which solute concentration can be measured. In a concentrated large unilamellar vesicle preparation, all solute molecules are within a few thousand angstroms of a membrane. Small molecules such as acetic acid or methylamine traverse these distances on the order of 10^{-3} s making membrane permeation rates on the order of milliseconds accessible.

Nuclear magnetic resonance (NMR) enables solutes in inner and outer compartments to be distinguished and solute concentrations can be rapidly measured (6). NMR provides an additional advantage in that permeation can be monitored under conditions in which all chemically distinct components are at equilibrium across the membrane. That is to say, there is no net flow of chemically distinct material during the course of the experiment. This property of the NMR experiment minimizes complications associated with studying permeation far from equilibrium. We will illustrate the application of NMR to permeation studies using the permeation of acetic acid through large unilamellar vesicle membranes. The permeation of weak acids and bases has been of interest because of their use in measurement of transmembrane pH gradients (7). Our choice of acetic acid, however, relates more to its expected high permeability and convenient proton NMR resonance.

Transport Theory

The rationale behind the NMR experiments is best understood in the context of nonequilibrium thermodynamics (8). It has been established that the transmembrane flow of a solution component can depend not only upon its own transmembrane chemical potential gradient but on the transmembrane chemical potential gradients of all other solution components. In situations where the solutions are ideal, the transmembrane chemical

potential gradients are linear and the gradients do not extend into the solution, the transmembrane flow through a unit cross section, J_i, can be expressed in terms of transmembrane concentration gradients, ΔCj:

$$\frac{AJ_i}{\overline{C_i}} = RT \sum_j L_{ij} \Delta Cj. \tag{1}$$

$\overline{C_i}$ is the average component concentration on the two sides of the membrane in the limit of small ΔC_i. A is the total surface area separating the solution compartments. L_{ij} are phemenological coupling constants, which express the extent to which the transmembrane concentration gradient in one component induces the permeation of other components. The system we will study is best approximated by two quaternary ideal solutions separated by the vesicle membrane. The solution components are solvent water, nearly impermeable solute (acetate anion), and two forms of permeable solute (neutral acetic acid) that are chemically identical but differ in nuclear spin properties. C_α is the solution concentration of permeable solute having nuclear spin in the α-state and C_β is the concentration of solute having nuclear spin in the β-state. We will show later that during the course of the NMR experiment the transmembrane gradient in α and β remain equal and opposite: $\Delta C_\alpha = -\Delta C_\beta$. In addition, we assume that C_α couples to solvent flow in exactly the same manner as C_β because we do not expect solvent-solute interactions to depend on nuclear spin properties. In the same light, we assume $L_{\alpha\alpha}$ and $L_{\beta\beta}$ are identical and there is no interaction between flows of dilute solutes, $L_{\alpha\beta} = L_{\beta\alpha} = 0$. Under these conditions the set of Eqs. 1 reduces to:

$$\frac{AJ_\alpha}{\overline{C_\alpha}} = L_{\alpha\alpha} RT \Delta C_\alpha$$

$$\frac{AJ_\beta}{\overline{C_\beta}} = L_{\beta\beta} RT \Delta C_\beta \tag{2}$$

Eq. 2 is consistent with the phemenological equation of flow used by Stein (9),

$$J_\alpha = P_\alpha \Delta C_\alpha. \tag{3}$$

The permeation coefficient, P_α, is therefore defined by:

$$P_\alpha = \frac{RT\overline{C_\alpha} L_{\alpha\alpha}}{A}. \tag{4}$$

NMR Theory

Two types of NMR experiments are performed: total lineshape analysis (TLA) and selective population transfer (SPT). To observe the flow of a molecule between the internal and the external vesicle compartments in either experiment, it is necessary that the internal and external chemical shifts be different. In our experiments, this is accomplished by adding a small amount of an impermeable paramagnetic ion (a shift reagent) to the external compartment (10). This procedure proved to be the simplest approach to differentiating the compartments, but it is not necessarily the only one available. Under some circumstances shifts from molecules in inner and outer compartments may be inherently different (11).

Because the SPT experiment is relatively new, we will describe it in detail. The intensity of either compartment's resonance, I, is proportional to the difference in α and β spin-state populations for the compartment. There is no net transmembrane flow of chemically distinct solute in our systems, so the variation in resonance intensity arises from opposing flows of magnetically distinct molecules:

$$\frac{dI}{dt} \alpha AJ_\alpha - AJ_\beta = AP_\alpha \Delta C_\alpha - AP_\beta \Delta C_\beta. \tag{5}$$

Because the permeation coefficients are identical for α and β spins, $P_s = P_\alpha = P_\beta$, and the compartment concentrations are related to the signal intensities through the compartment volumes V1 and V2, we have

$$\begin{aligned} \frac{d\,I1}{dt} &= \frac{AP_s}{V2} I2 - \frac{AP_s}{V1} I1 \\ \frac{d\,I2}{dt} &= \frac{AP_s}{V1} I1 - \frac{AP_s}{V2} I2. \end{aligned} \tag{6}$$

The numbers after the terms V and I are compartment labels.

The SPT experiments provide for flow of magnetically distinct molecules without flow of total solute. This condition is attained by inverting spin populations in one compartment with a long, low-power rf pulse at the frequency of the solute resonance. The rf pulse causes a one for one exchange of α spins for β spins thus insuring that $\Delta C_\alpha = -\Delta C_\beta$. A spectrum taken directly after the pulse has the resonance for one compartment inverted while the resonance for the other compartment remains unperturbed. After inversion neither compartment is at thermal equilibrium: the inverted one because of a nonequilibrium spin population that recovers by nuclear relaxation and both because of concentration differences that recover by solute flow. The intensity variation will depend on both the longitudinal relaxation times $T_1 1$ and $T_1 2$ and on solute permeation.

$$\begin{aligned} \frac{d\,I1}{dt} &= \frac{AP_s}{V2} I2 - \frac{AP_s}{V1} I1 - \frac{1}{T_1 1} (I1 - I_\infty 1) \\ \frac{d\,I2}{dt} &= \frac{AP_s}{V1} I1 - \frac{AP_s}{V2} I2 - \frac{1}{T_1 2} (I2 - I_\infty 2) \end{aligned} \tag{7}$$

$I1_\infty$ and $I2_\infty$ are the resonance intensities after all transmembrane flows and nuclear relaxation flows have reached equilibrium. Because of the permeation term in Eq. 7 the inverted line will initially grow at the expense of intensity in the unperturbed line. Eventually both lines recover equilibrium intensities according to the nuclear relaxation terms. The quantities $AP_s/V1$ and $AP_s/V2$ have dimensions of s^{-1} and are interpreted as reciprocal average lifetimes of solute in the two compartments. Substitution of these quantities by $1/\tau 1$ and $1/\tau 2$ and M_z for I yields the modified Bloch equations for the longitudinal magnetization component in a chemically exchanging system (12). Procedures for selectively inverting NMR resonances and analysis of the subsequent time evolution of intensities have been previously described for molecular systems involved in conformational equilibria (13–15).

These procedures will be extended to systems where the exchange process is transmembrane flow of solute molecules to extract values of $\tau 1$, $\tau 2$, $T_1 1$, and $T_1 2$.

Solutes can also be labeled according to the characteristics of their transverse magnetization components. The TLA experiment labels solute molecules according to the precessional frequency of the transverse spin magnetization. An analysis similar to that outlined for the SPT experiment leads to modified Bloch equations for the transverse components. The results state that the permeation rate will manifest itself in broadening and coalescence of the inner and outer resonances (16).

TLA and SPT are complimentary for membrane permeation study. TLA experiments can detect lifetimes in the range of 10 ms, but inherent solute line widths in membrane preparations are often so broad that TLA experiments are insensitive to compartment lifetimes much beyond 100 ms. SPT experiments, on the other hand, are sensitive to compartment lifetimes similar in magnitude to longitudinal relaxation times (several seconds for small molecules). Taken together, SPT and TLA experiments provide a method of measuring permeation rates, some of which have been previously inaccessible due to unstirred layer effects or to the long dead times associated with labeling techniques.

In addition to illustrating the use of TLA and SPT for membrane permeation studies, the acetic acid permeation work reported here can provide some interesting insight into the mechanism of acetic acid permeation.

MATERIALS AND METHODS

Preparation and Characterization of Vesicles

Large unilamellar vesicles were prepared by ether injection using an apparatus similar to that described by Deamer and Bangham (5). A 30-ml diethyl ether solution was prepared from 60 mg egg yolk phosphatidylcholine (17), 0–10 mg phosphatidic acid (18), and 1 ml of methyl alcohol to completely dissolve the phospholipids. Using a peristaltic pump, this solution was injected into 5 ml of deuterated sodium acetate buffer (0.01–0.2 M) containing a small amount of the chemical shift standard, 3(trimethylsilyl) propanesulfonic acid sodium salt (DSS), at a rate of 0.1 ml/min, while maintaining aqueous solution temperature at 60°C. Upon completion of ether injection, the vesicle suspension was concentrated by twofold. For samples that contained no phosphatidic acid concentration was effected by pelleting the vesicles at centrifugal fields of $< 1{,}000$ *g*. Samples that contained phosphatidic acid were concentrated by ultrafiltration using a Millipore ultrafiltration apparatus and Pellicon PSED molecular filters (Millipore Corp., Bedford, Mass.). Residual ether and methanol were then removed from the concentrate by dialysis against the buffer used in the injection procedure. NMR spectra of the sample after dialysis show the residual ether to be < 1 mM and residual methanol to be < 4 mM in samples where the lipid concentration is 20 mM. Inner and outer acetic acid resonances were resolved by adding (to the dialyzed samples) 0.02 to 0.10 mol $Pr(NO_3)_3$ per mol of total sodium acetate. After completion of the NMR experiments the p^2H and concentration of phospholipid were determined. The reported p^2H was obtained by adding 0.4 U (19) to the pH meter reading. The phospholipid concentration, [PL] (in micromoles of phospholipid per milliliter), was determined according to the method of Fiske and SubbeRow (20).

The membrane surface area:entrapped volume ratio, $A{:}V1$ (in centimeters^{-1}), was calculated for each sample using

$$\frac{A}{V1} = [PL]\,\frac{V1 + V2}{V1}\,(6.0 \times 10^{17})(34 \times 10^{-16}),$$

assuming all of the lipid forms large unilamellar vesicles in which each lipid molecule occupies 68 Å of monolayer surface area (21). The entrapped:total volume ratio, $V1:(V1+V2)$, is equal to the ratio of the inner compartment resonance area to the total resonance area, assuming the solute concentration to be the same in each compartment.

Collection of NMR Data

All NMR data were collected with a Bruker HX270 spectrometer (Bruker Instruments, Inc., Billerca, Mass.) interfaced with a Nicolet BNC-12 computer (Nicolet Instrument Corp., Madison, Wisc.). The spectrometer was operated in the Fourier transform mode at 270 MHz for ^{1}H nuclei. The sample temperature was maintained by the standard Bruker variable temperature accessory to ± 2°C.

In the TLA experiments, the changes in lineshape associated with temperature-induced modulation of the permeation rate were observed by recording a series of spectra at different temperatures for each sample. Each spectrum was the averaged result of 20–50 acquisitions separated by 7–10-s pulse delays to obtain intensities that quantitatively reflect the compartment solute populations. The spectra were Fourier transformed and phased with the Nicolet computer and transferred to a PDP 11/45 computer (Digital Equipment Corp., Maynard, Mass.) where the total lineshape fitting took place.

The SPT experiments were performed using standard Nicolet Fourier Transform software, a Nicolet 293 I/0 controller, and a computer-controlled frequency synthesizer to generate a selective pulse in a manner similar to that described previously (13). The selective pulse width was between 10 and 25 ms and was adjusted for each sample to attain optimum selective inversion (70–90%) of the inner compartment resonance. It was followed by a variable delay time and a 90° observation pulse. Signals from 10 to 40 such pulse trains were averaged. The relaxation behavior was adequately described by recording spectra at 10–15 delay times. Fully relaxed control spectra were collected during SPT data acquisition to ascertain if significant irreversible changes were occurring.

Determination of Solute Compartment Lifetimes

The lineshape in the TLA experiments depends on the inner compartment lifetime, $\tau 1$, as well as the total intensity, the fraction of the total solute residing in each compartment, the chemical shifts of the inner and outer resonances, and the line widths in the absence of exchange. These contributions were estimated by Lorentzian line fitting the low temperature spectral data where permeation is slow and does not affect the lineshape. For more rapid permeation, the lineshape is specified by functions outlined by Piette and Anderson (22) and Johnson (23). $\tau 1$ (or $\tau 2$) was extracted by multidimensional fitting using these equations and a modified gradient search procedure similar to the one outlined by Bevington (24). In some cases, multidimensional fitting was not necessary because permeation was sufficiently slow to cause broadening without coalescence throughout the range of temperatures studied. Compartment lifetimes for each sample were extrapolated to a common temperature (280 K) by plotting $\ln 1/\tau 1$ vs. the inverse absolute temperature.

The uncertainty in the $\tau 1$ value arising from a particular spectrum was estimated by holding all the parameters but $\tau 1$ constant and calculating the increment in $\tau 1$ that would increase the unweighted mean squared difference between the observed and the simulated lineshape by a factor of two. These uncertainties were propagated by the method of limiting slopes to obtain the uncertainty in the extrapolated $\tau 1$ value at 280 K.

In the SPT experiments, the resonance intensities and line widths were determined with the Nicolet Fourier Transform program. Because the inner and outer lines had different widths, the temporal variation of integrated area was used to define the relaxation. The theoretical relaxation behavior is given by Eqs. 1 and 2 of reference 13. The behavior depends on seven parameters: the equilibrium line intensities, the initial intensities, the inner and outer relaxation times, and one compartment lifetime. The equilibrium intensities were determined from the totally relaxed spectra. The five remaining parameters were fit to the data by two procedures to yield the compartment lifetimes. One procedure involved multidimensional fitting with a program similar to that used for the TLA data. The other procedure involved separation of the exponential terms of Eqs. 1 and 2 of reference 13 by logarithmic

plotting. All the SPT experiments were performed at 280 K. The reported uncertainties in $\tau 1$ are the increment which changes, by a factor of two, the unweighted mean squared difference between the observed and simulated relaxation curves.

RESULTS

Vesicle Characterization

Fig. 1 A shows the ^1H spectrum of a typical preparation of large unilamellar vesicles with the acetic acid resonance at 1.9 ppm and the $^1H^2HO$ resonance at 4.9 ppm relative to DSS. Addition of $Pr(NO_3)_3$ produces two peaks in the methyl region (Fig. 1 B). The resonance at 2.8 ppm arises because the Pr^{3+} and acetate in the outer compartment form a labile complex in which the Pr^{3+} induces a downfield dipolar shift of the acetate resonance. Exchange of acetate between the protonated, unprotonated, and Pr^{3+} bound forms is rapid enough to average the outer resonance to a single line. The Pr^{3+} ion does not permeate the membrane so acetic acid in the inner compartment resonates at 1.9 ppm.

Our preparations yielded entrapped:total volume ratios ranging from 0.20 to 0.50. When stored in the absence of Pr^{3+}, this ratio for a given sample remained constant for several days, reflecting the inherent stability of the vesicle preparation. After Pr^{3+} addition this ratio decreased more rapidly for phosphatidic acid containing vesicles, but generally $< 20\%$ in 1 h, the time period of most SPT or TLA experiments. Increased rupture in the presence of phosphatidic acid and a trivalent ion is not unexpected in view of Ca^{2+}-induced fusion observed for similar vesicle systems.[1]

The trapping efficiency, as defined by Deamer and Bangham (5), η, (microliters of

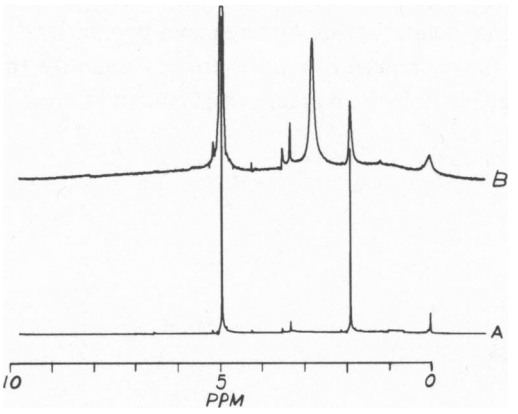

FIGURE 1

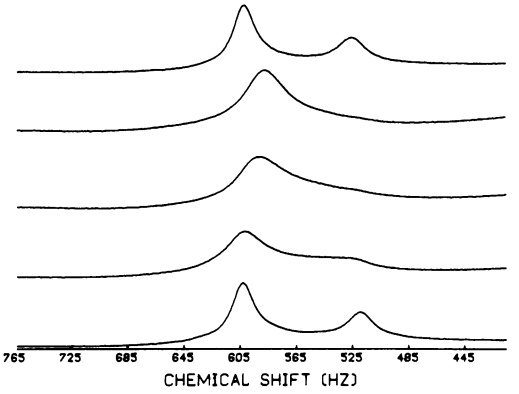

FIGURE 2

FIGURE 1 (A) ^1H 270 MHz spectrum of a large unilamellar vesicle preparation. 0.10 M NaAC, p^2H 6.7, 7°C. (B) Spectrum in A after addition of $Pr(NO_3)_3$ to 5 mM.

FIGURE 2 Total lineshape of the acetate resonances as a function of temperature at p^2H 5.5, 0.1 M NaAC. Bottom to top: 7, 35, 45, 55, 7°C. Chemical shift scale in hertz upfield of DSS. 1 ppm = 270 Hz.

[1]Liao, M. J., and J. H. Prestegard. 1979. Fusion of the phosphatidic acid-phosphatidylcholine mixed lipid vesicles. Submitted for publication.

entrapped solution per micromoles of phospholipid), reflects the reproducibility of the preparation procedure. The average value and standard deviation of η based on the 14 samples used for NMR permeation measurements is 12 ± 4. The observed trapping efficiency can also be used to determine the extent to which the vesicles are unilamellar. Given that a vesicle is a spherical shell of radius r (Å), and each lipid molecule occupies 68 Å^2 of surface area (21), the trapping efficiency can be expressed as $(68r \cdot 10^{-4})/\phi$, where ϕ is the average number of bilayers per spherical shell. Analysis of electron micrographs indicates the average value of r varies from 1,000 to 4,000 Å. The corresponding range in ϕ is 0.6–2.0, indicating the average sample is predominantly composed of unilamellar vesicles.

Permeation Rates

A representative set of TLA data is presented in Fig. 2. Increasing temperature induces more rapid permeation causing the inner and outer resonances to broaden and coalesce. Our ability to reproduce the low temperature spectrum at the conclusion of the series ensures that the spectral changes are a result of reversible modulation of the permeation rate by temperature and not the result of an irreversible vesicle transformation. Fig. 3 shows the attainable agreement between best fit simulation and the data. The inside compartment lifetime varies from 15 ms at 7°C to 2.5 ms at 65°C for this particular data set. In all cases, the Arrhenius plots were linear and their slopes could be used to determine the activation energy for permeation from inner compartment to outer compartment. The observed activation energy averaged over all the TLA experiments was 10 ± 4 kcal/mol.

SPT spectra plotted in the order in which they were collected are shown in Fig. 4. The reproducibility of the intermediate long delay spectra show that the sample's properties are not changing during the course of data acquisition. The intensity decay in the outer resonance at short delay times results from transfer of inner solute having inverted spin populations to the outer compartment via permeation. SPT fitting procedures were used to quantify the permeation rates. The example presented in Fig. 5 is fit with an inner compartment lifetime of 0.46 s.

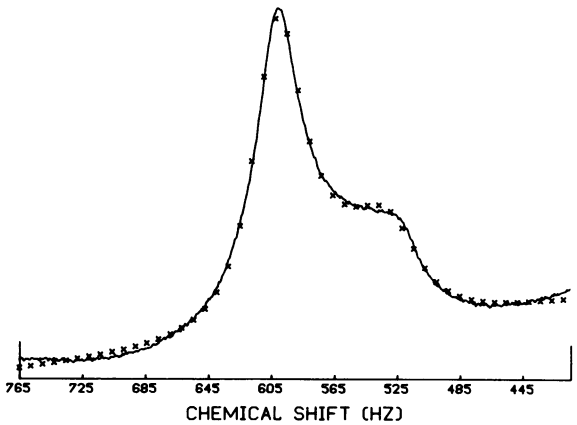

FIGURE 3 Observed TLA data (solid line) and best fit simulation (X) for 35° spectrum in Fig. 2. $\tau 1$ equals 5.0 ms for this fit.

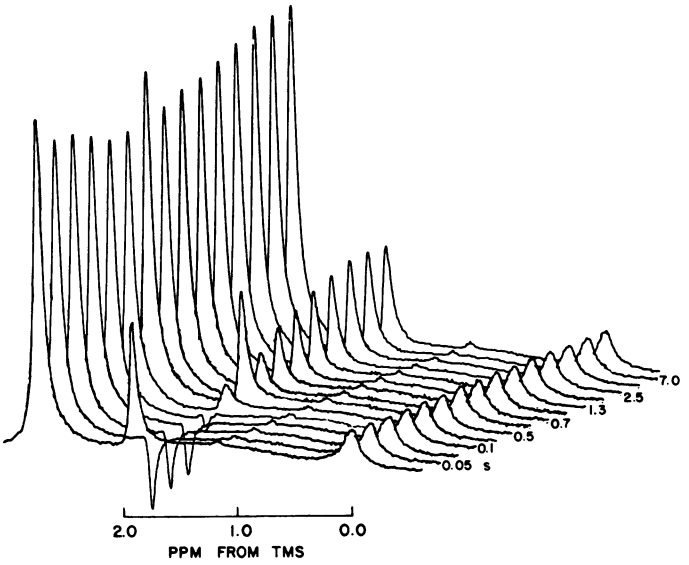

FIGURE 4 Stacked plot of SPT data. Conditions are similar to Fig. 1. Delay times appear to the right of every other spectrum. TMS, tetramethylsilane.

Permeation rate measurements were performed by SPT and TLA from 5.4–6.9 p^2H, for samples having total acid concentrations from 0.01 M to 0.2 M and for membranes composed of 0–15 wt % phosphatidic acid. The solute's inner compartment lifetime at 7°C is 1 s at p^2H 6.9 and progressively decreases with p^2H to 0.01 s at p^2H 5.4. Variation in phosphatidic acid and solute concentration had a minimal effect on the observed solute compartment lifetimes.

DISCUSSION

The authors, who have reported acetic acid model membrane permeation studies (25, 26), conclude that permeation is rapid and that protonated acetic acid, HAC, permeates preferentially to the anion, AC^-. However, a numerical value for the permeation coefficient

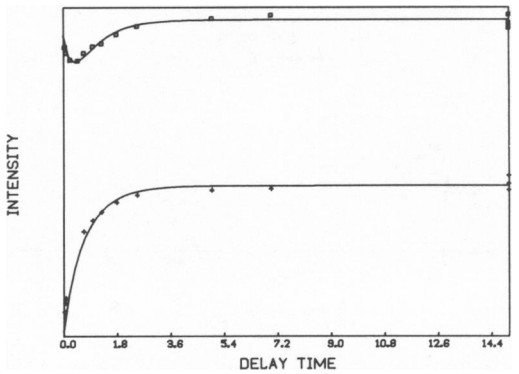

FIGURE 5 Comparison of observed relaxation (□, outside resonance; +, inside resonance) and best fit simulation (solid line) for data appearing in Fig. 4.

was not reported. Our finding that the solute compartment lifetimes shorten as the p^2H is decreased supports the qualitative results. A quantitative analysis of the p^2H dependence of the solute compartment lifetimes allows us to report the numerical value of the permeation coefficient for deuterated acetic acid, ^{2}HAC. The analysis is briefly outlined as follows. Eq. 7 was derived assuming all the molecules giving rise to the resonances were permeable. For acetic acid, this is not the case, because the rapid protonation equilibrium averages the resonances from ^{2}HAC and AC^- to a single line. The relative amounts of ^{2}HAC and AC^-, and, therefore, the relative contributions to the compartment resonances are determined by the p^2H of the solutions and the acid dissociation constant, K_A. Assuming that ^{2}HAC is the only permeable solute, we expect $\tau 1$ and $\tau 2$, which define the compartment lifetimes of total acid (HAC + AC^-), to become shorter as the p^2H is lowered and a larger percentage of the total acid is in a permeable form. Taking the permeation coefficient for ^{2}HAC, $P_{^2HAC}$, as a p^2H independent value, and correcting Eq. 7 for the variation in permeable solute with p^2H, we obtain the following relationship between the inner compartment lifetime, $\tau 1$, and the p^2H:

$$\tau 1 = \frac{1}{P_{^2HAC}} \frac{V1}{A}\left[\frac{K_A}{[^2H^+]} + 1\right]. \tag{9}$$

Our data are presented as a plot of $\tau 1$ vs. $V1/A\,[K_A/[^2H^+] + 1]$ in Fig. 6 using $K_A = 0.755 \times 10^{-5}$ (27). The data fit a straight line agreeing with Eq. 9. This agreement supports the assumption that only ^{2}HAC is permeable. The slope of the plot yields a value of $5 \pm 2 \times 10^{-4}$ cm/s for $P_{^2HAC}$ at 7°C. Points included on the plot also show permeation rate to be insensitive to total acetic acid concentration and to the presence of phosphatidic acid.

Our ability to quantify the acetic acid permeation illustrates the use of NMR rate measurements in the study of membrane permeation phenomena when the permeation rates are too fast to be measured within the dead time of the more classical procedures. This series

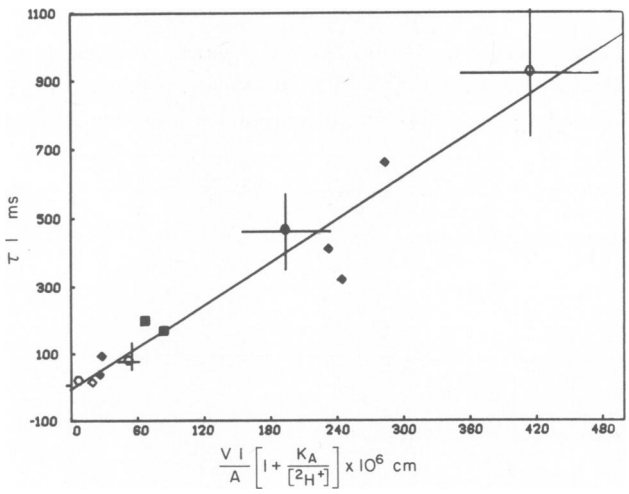

FIGURE 6 Plot of observed inside lifetime, $\tau 1$ vs. $V1/A\,[1 + K_A/(^2H^+)]$; (○) 0.2 M NaAC; (◇) 0.1 M NaAC; (□) 0.01 M NaAC. Open characters: pure egg phosphatidylcholine vesicles. Closed characters: mixed phosphatidic acid-phosphatidylcholine acid vesicles. Solid line is the best unweighted least squares fit to all the data points. Representative error bars are included on several points.

of experiments has resulted in observation of compartment lifetimes from 1 ms to 1 s. In addition to illustrating the use of NMR permeation measurements, this work has provided some unexpected insight into the molecular mechanism of acetic acid permeation. The key observations that assist in discussing the permeation mechanism are the numerical value of the ^{2}HAC permeation coefficient and its lack of dependence on total acid concentration (see Fig. 6).

Because of the solute and membrane complexity, the molecular permeation process is viewed by many authors within the framework of a rather simple model. We intend to follow this procedure by comparing our measured permeation coefficient to one calculated from a model. The model we choose takes the membrane, separating the two solution compartments, to be a hydrophobic continuum of width, l, with the physico-chemical properties similar to those of common nonpolar solvents. The permeation proceeds via a rapid partitioning of the permeant into the hydrophobic region at one interface followed by rate limiting diffusion to the opposite interface, and finally by release to the opposite compartment via the partitioning process. For this model the permeation coefficient can be expressed as:

$$P = \frac{DR}{l}, \tag{10}$$

where D is the diffusion coefficient for the permeant solute in the membrane, R is the partition ratio of the solute between membrane and aqueous phases and l is the thickness of the membrane. D is calculated with the Stokes-Einstein formula using 3 Å for the effective acetic acid radius and a viscosity, 138 cp, similar to that of olive oil at 10°C (28). The partition ratio for the acetic acid in an oil-water system, 0.03, gave an estimate for R (29). The thickness of the membrane is taken to be 50 Å. The calculated permeation coefficient is 3×10^{-3} cm/s, an order of magnitude larger than our measured value. Because we have been conservative in estimating parameters for the calculation, we believe the difference to be significant and conclude that the simple model does not adequately describe the acetic acid permeation process.

One of the more suspect estimates is the one for D, because it has been suggested that the hydrocarbon is "polymeric" rather than continuous in nature (30). Observed translational diffusion coefficients in polymeric materials are generally smaller than diffusion coefficients predicted by a continuum model and may reduce the predicted permeation coefficient by as much as a factor of 10. A less conservative choice of R, such as that for octanol-water partitioning would (29), however, put even the polymeric model out of contention and force further consideration of other models.

The existence of acetic acid dimers in aqueous and nonpolar media suggests that the acetic acid dimer could play a role in the acetic acid permeation mechanism. However, apparently the dimer does not play a part in the process, because the permeation rate remains constant when the membrane dimer:monomer concentration ratio is changed by changing the total acid concentration at constant pH. A more quantitative consideration of dimerization using published partition ratios and dimerization constants from reference (29), indicates that, for our samples, <10% of the total membrane-dissolved acetic acid would be in the form of dimers.

We believe that further modification of the model requires relieving the constraint that permeant diffusion in the hydrocarbon region limits the permeation rate. In the case of acetic

acid permeation, it is likely that the step in which the permeant crosses the interfacial region between aqueous solution and hydrocarbon occurs more slowly than does diffusion within the hydrocarbon. Crossing of the interface may involve one or more dehydration steps for the acetic acid molecule or it may involve considerable steric hindrance at the headgroup level. The presence or absence of phosphatidic acid would be expected to alter the nature of headgroup region. Although the percentage of phosphatidic acid in our samples is low, the absence of a pronounced effect on permeation rates makes dehydration the more likely candidate. Clearly more investigation into this possibility is warranted. We feel that NMR methodology of the type illustrated in this article will be useful in pursuing further investigations.

We are grateful for the support provided by grant GM19035 and by the Biotechnology Resources Program of the National Institutes of Health through the Southern New England High Field NMR Facility (RR-798).

Received for publication 1 March 1979.

REFERENCES

1. THOMPSON, T. E., and F. A. HENN. 1970. Experimental phospholipid model membranes. *In* Membranes of Mitochondria and Choloroplasts, E. Racker, editor. Van Nostrand Reinhold Co., New York.
2. JAIN, M. K. 1972. The Bimolecular Lipid Membrane: A System. Van Nostrand Reinhold Co., New York. Chapter 5.
3. TIEN, H. T. 1974. Bilayer Lipid Membranes: Theory and Practice. Marcel Dekker, Inc., New York. Chapter 6.
4. ANDREOLI, T. E., and S. L. TROUTMAN. 1971. An analysis of unstirred layers in series with "tight" and "porous" lipid bilayer membranes. *J. Gen. Physiol.* **57**:464–478.
5. DEAMER, D., and A. D. BANGHAM. 1976. Large volume liposomes by an ether injection procedure. *Biochim. Biophys. Acta.* **443**:629–634.
6. CRAMER, J. A., and J. H. PRESTEGARD. 1977. NMR studies of pH-induced transport of carboxylic acids across phospholipid vesicle membranes. *Biochem. Biophys. Res. Commun.* **75**:295.
7. JOHNSON, R. G., N. J. CARLSON, and A. SCARPA. 1978. pH and catecholamine distribution in isolated chromaffin granules. *J. Biol. Chem.* **253**:1512–1521.
8. KATCHALSKY, A., and P. F. CURRAN, 1965. Nonequilibrium Thermodynamics in Biophysics. Harvard University Press. Cambridge, Mass. Chapter 10.
9. STEIN, W. D. 1967. The Movement of Molecules Across Cell Membranes. Academic Press, Inc., New York. Chapter 2.
10. CHRZESZCZYK, A., A. WISHNIA, and C. S. SPRINGER, Jr. 1976. Hyperfine induced splitting of free solute nuclear magnetic resonances in small phospholipid vesicle preparations. *ACS Symp. Ser.* **34**:483–498.
11. KANTOR, H. L., and J. H. PRESTEGARD. 1978. Fusion of phosphatidylcholine bilayer vesicles: role of free fatty acid. *Biochemistry.* **17**:3593.
12. MCCONNELL, H. M. 1958. Reaction rates by nuclear magnetic resonance. *J. Chem. Phys.* **28**:430–431.
13. ALGER, J. R., and J. H. PRESTEGARD. 1977. Investigation of peptide bond isomerization by magnetization transfer NMR. *J. Magn. Reson.* **27**:137–141.
14. CAMPBELL, I. D., C. M. DOBSON, R. G. RATCLIFFE, and R. J. P. WILLIAMS. 1978. Fourier transform NMR pulse methods for the measurement of slow exchange rates. *J. Magn. Reson.* **29**:397–417.
15. DAHLQUIST, F. W., K. J. LONGMUIR, and R. B. DUVERNET. 1975. Direct observation of chemical exchange by a selective pulse NMR technique. *J. Magn. Reson.* **17**:406–410.
16. BOVEY, F. A. 1969. Nuclear Magnetic Resonance Spectroscopy. Academic Press, Inc., New York. Chapter VII.
17. SINGLETON, W. S., M. S. GRAY, M. L. BROWN, and J. L. WHITE. 1965. Chromatographically homogeneous lecithin from egg phospholipids. *J. Am. Oil Chem. Soc.* **42**:53.
18. PAPAHADJOPOULOS, D., and N. MILLER. 1967. Phospholipid model membranes I. Structural characteristics of hydrated liquid crystals. *Biochim. Biophys. Acta.* **135**:624–638.
19. GLASOE, P. K., and F. A. LONG. 1960. Use of glass electrodes to measure acidities in deuterium oxide. *J. Phys. Chem.* **64**:188–190.
20. BARTLETT, G. R. 1959. Phosphorous assay in column chromatography. *J. Biol. Chem.* **234**:466–468.

21. SHIPLEY, G. G., 1973. Recent x-ray diffraction studies of biological membranes and membrane components. *In* Biological Membranes. D. Chapman and D. F. H. Wallach, editors. Academic Press. **2**:12.
22. PIETTE, L. H., and W. A. ANDERSON, 1959. Potential energy barrier determination for some alkyl nitrates by nuclear magnetic resonance. *J. Chem. Phys.* **30**:899.
23. JOHNSON, C. S., JR. and C. G. MORELAND. 1973. The calculation of NMR spectra for many site exchange problems. *J. Chem. Ed.* **50**:477–483.
24. BEVINGTON, P. R. 1969. Data Reduction and Error Analysis for the Physical Sciences. McGraw-Hill Book Co., New York. 219.
25. SINGER, M. A., and A. D. BANGHAM. 1971. The consequences of inducing salt permeability in liposomes. *Biochim. Biophys. Acta.* **241**:687–692.
26. SINGER, M. A. 1973. Transfer of anions across phospholipid membranes. *Can. J. Physiol. Pharmacol.* **51**:523–531.
27. KORMAN, S. and V. K. LAMER, 1936. Detuerium exchange equilibria in solution and the quinhydrone electrode. *J. Am. Chem. Soc.* **58**:1396.
28. Handbook of Chemistry and Physics. 56th edition. 1975. Chemical Rubber Co. F-54.
29. LEO, A., C. HANSCH, and D. ELKINS. 1971. Partition coefficients and their uses. *Chem. Rev.* **71**:557.
30. LIEB, W. R., and W. D. STEIN. 1971. The molecular basis of simple diffusion within biological membranes. *Curr. Top. Membr. Transp.* **2**:1–39.